Faraday rotation spectra of bismuth-substituted ferrite garnet films with in-plane magnetization

L. E. Helseth, R. W. Hansen, E. I. Il'yashenko, M. Baziljevich, and T. H. Johansen
Department of Physics, University of Oslo, P.O. Box 1048 Blindern, N-0316 Oslo, Norway
(Received 30 April 2001; published 2 October 2001)

Single crystal films of bismuth-substituted ferrite garnets have been synthesized by the liquid phase epitaxy method where gadolinium gallium garnet substrates are dipped into the flux. The growth parameters are controlled to obtain films with in-plane magnetization and virtually no domain activity, which makes them excellently suited for magnetooptic imaging. The Faraday rotation spectra were measured across the visible range of wavelengths. To interpret the spectra we present a simple model based on the existence of two optical transitions of diamagnetic character, one tetrahedral and one octahedral. We find excellent agreement between the model and our experimental results for photon energies between 1.77 and 2.53 eV, corresponding to wavelengths between 700 and 490 nm. It is shown that the Faraday rotation changes significantly with the amount of substituted gallium and bismuth. Furthermore, the experimental results confirm that the magnetooptic response changes linearly with the bismuth substitution.

DOI: 10.1103/PhysRevB.64.174406 PACS number(s): 75.70.Ak, 78.20.Ls

I. INTRODUCTION

Bismuth-substituted ferrite garnets (Bi:FGs) are well known to have a giant magnetooptical response.[1–9] For this reason, they have found widespread use as spatial light modulators, optical switchers and optical isolators. Recently it was realized that Bi:FG films with in-plane magnetization allow visualization and detection of magnetic fields.[10,11] As basic sensors for magnetooptic imaging they have been used extensively in studies of magnetic flux in superconductors, domain formation in magnetic materials, currents in microelectronic circuits and recorded patterns in magnetic storage media.[12–18] In spite of their successful applications, relatively few studies have been directed towards the understanding of the magnetooptical properties of Bi:FG films themselves. Of particular interest here is the behavior and optimization of the Faraday rotation spectra.

The dodecahedral sites in garnet crystals can accept several rare-earth ions, and each substitution seems to introduce its own special modification in the properties. All of the Bi^{3+}, Ce^{3+}, and Pb^{2+} have been shown to increase the Faraday rotation within certain wavelength intervals.[18–22] With Bi^{3+} a very strong Faraday rotation is obtained in the visible range, which together with the fact that the grown crystals are nearly transparent, make them by far the most frequently used material for magnetooptic imaging. For this application an important point is also that the films with in-plane magnetization are essentially free of magnetic domains.

The understanding of the magnetooptical spectra in garnets is based on the knowledge of the spin orbit interaction in these materials. The spin orbit interaction generally causes a splitting of both the ground and excited states. However, in many cases it is possible to assume splitting of one of the states. Then only two situations are possible. (i) A paramagnetic transition, which is due to a orbital degenerate ground state with a singlet excited state. (ii) A diamagnetic transition, which is due to a orbital singlet ground state with a spin orbit split excited state. Since the paramagnetic and diamagnetic transitions have quite different line shapes,[18] it should in principle be possible to distinguish between isolated diamagnetic and paramagnetic transitions, and therefore obtain a correct interpretation of the spectra. However, Bi:FG materials have several transitions within the UV and visible region, which complicates the interpretation considerably. This has led to some controversy regarding the kind of transitions involved, and therefore how to reproduce the spectra theoretically.[9,23–27]

Simsa *et al.* measured the Faraday rotation of liquid phase epitaxy (LPE) grown Bi:FG films with small substitutions of bismuth.[9] To interpret the spectra, they introduced one diamagnetic and several paramagnetic transitions. In this way they were able to correctly predict the behavior of the spectra in the visible and near-infrared region. However, there were still some deviations between experimental and theoretical data when the bismuth substitution increased. More recently, Matsumoto *et al.* measured the Faraday rotation for Bi:FG films made by the gel method.[26,27] Here reasonable agreement between the experimental data and the theoretical predictions was obtained with four paramagnetic transitions in addition to the four diamagnetic ones. However, the inclusion of paramagnetic transitions was not explained. Actually, Dionne and Allen questioned whether paramagnetic transitions can account for the contribution from Bi, since the strong superexchange field of the spin degeneracy exclude Zeeman splitting of the ground state, thus leaving a spin singlet ground state.[24]

In this paper we report experiments and modelling of the Faraday rotation spectra in Bi:FG films suitable for magnetooptic imaging. To that end we have grown a series of Bi:FG films using the LPE technique, and characterized their chemical composition. The Faraday rotation spectra have been measured for photon energies between 1.77 and 2.53 eV, corresponding to wavelengths between 700 and 490 nm. It is shown that the Faraday rotation changes significantly with the amount of substituted gallium and bismuth. Furthermore, the comparison of experimental and theoretical data confirms that the magnetooptic response changes linearly with the bismuth substitution.

TABLE I. The thickness and chemical composition of the four samples.

Sample No.	Lu	Y	Bi	Pb	Fe	Ga	t (μm)
1	1.619	0.625	0.683	0.064	3.842	1.144	7.5
2	2.141	0	0.796	0.065	3.887	1.088	4.0
3	2.166	0	0.874	0.037	3.937	0.969	4.0
4	2.186	0	0.818	0.062	3.744	1.170	2.6

II. EXPERIMENT

A. Sample preparation

Single crystal films of Bi:FG were grown by isothermal LPE from $Bi_2O_3/PbO/B_2O_3$ flux onto (100) oriented gadolinium gallium garnet (GGG) substrates. The growth takes place while the 30 mm diameter substrate is dipped into the melt contained in a Pt crucible. During the growth, the parameters could be controlled to create low magnetic coercivity and in-plane magnetization in the garnet films. The thickness of the films was measured using a scanning electron microscope (SEM), and their composition determined with an electron microprobe (EMP). Thicknesses and compositions of four selected samples are listed in Table I. For sample 1, 2, and 4 the film was grown on only one side of the substrate, whereas sample 3 has a 2 μm thick film on both sides of the substrate.

From Table I one sees that the films can be represented by the following general formula:

$$\{Lu_{3-x-y-z}Y_yBi_xPb_z\}[Fe_{2-u_a}Ga_{u_a}](Fe_{3-u_d}Ga_{u_d})O_{12},$$

where { } indicates the dodecahedral site, [ ] the octahedral site, and ( ) the tetrahedral site. Note that only the total gallium content $u=u_a+u_d$ can be extracted from the EMP, and to determine u_a and u_d separately other techniques such as neutron spectroscopy must be applied. Usually, these techniques require bulk samples, and are not very useful for thin films. The films also contain small amounts of Pb, typically of the order of $z=0.05$. In the theoretical analysis of the Faraday spectra, we will neglect the contribution from Pb.

B. Faraday spectra measurements

The Faraday rotation as a function of wavelength at room temperature was measured using a setup consisting of a monochromatic light source, polarizer, two magnetic Helmholtz coils, sample, analyzer, and detector. A schematic drawing is shown in Fig. 1. The Helmholtz coils produce a magnetic field up to 1.1 kOe along the optical axis, which makes it possible to saturate the Faraday rotation of the sample. In this work all the samples were brought into saturation during the measurements. The Faraday rotation angle was measured as[9]

$$\Theta_F=\frac{\theta_{\rm tot}-\theta_{\rm sub}}{t}, \quad (1)$$

where $\theta_{\rm tot}$ is the Faraday rotation measured for the combined film and substrate, $\theta_{\rm sub}$ is the Faraday rotation of the bare substrate, and t is the thickness of the film. The substrates used in this study are 0.5 mm thick, and give only a small contribution of $\sim 0.1°$. In the present study we found that interference effects due to finite thickness as well as the Faraday ellipticity could be neglected. The Faraday rotation has been measured across the useful visible wavelength range with an accuracy of 0.05 degrees. The wavelength was determined within ± 1 nm.

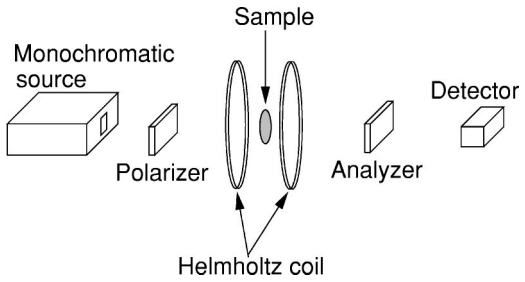

FIG. 1. Setup for measurement of the Faraday spectra. The analyzer is set at 45° from extinction to maximize the signal. To polarize the light we use a sheet polarizer, whereas the analyzer is a Glan-Thompson prism. Together they have an extinction ratio of $\sim 10^{-4}$. To measure the signal we used an ordinary silicon detector with 3×3 mm^2 active area.

Shown in Figs. 2–4 is the observed Faraday rotation as a function of energy for samples 1–4. Here Θ_F is denoted by negative numbers since we follow the sign-convention of Refs. 9,24,25. One sees that for samples 1–3, the magnitude of Θ_F increases monotonically with the photon energy. The largest rotation was found in sample 3 at 2.43 eV where $\Theta_F=4.6$ deg/μm. Since sample 4 is relatively thin, we were able to measure the spectrum up to 2.53 eV without reducing the accuracy of the measurement. This revealed a peak in the spectrum near 2.45 eV, where $\Theta_F=4.1$ deg/μm.

III. THEORY

Our analysis of the Faraday rotation spectra is based on the molecular-orbital energy-level diagram of Dionne and

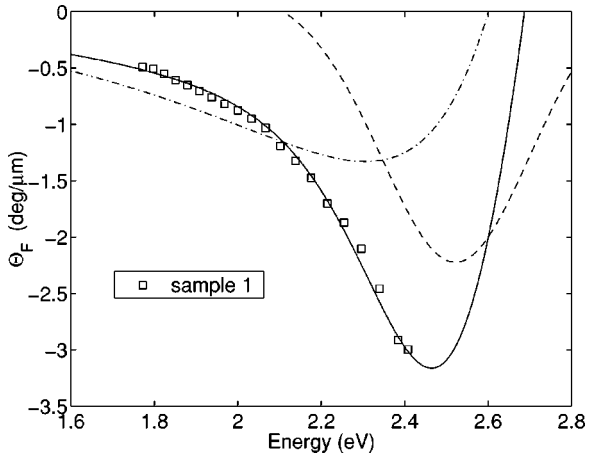

FIG. 2. The Faraday rotation for sample 1. The squares are the experimental data whereas the solid line represents the theoretical fit. The dashed and dash-dotted lines represent the contribution from the tetrahedral and octahedral transitions, respectively.

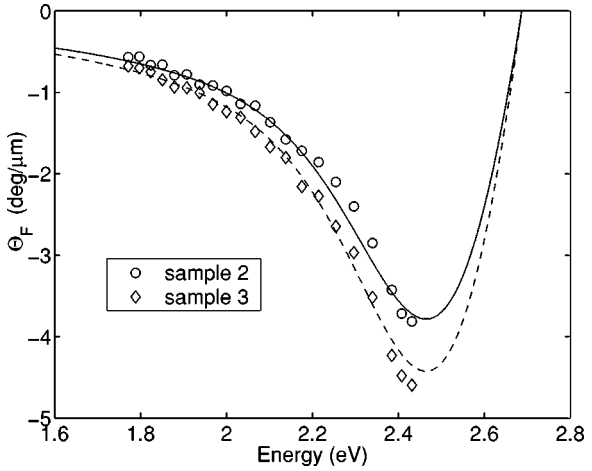

FIG. 3. The Faraday rotation for samples 2 (circles) and 3 (diamonds). The solid and dashed lines represent the theoretical fit for samples 2 and 3, respectively.

Allen,[23] shown in Fig. 5. The basic mechanism behind the enhanced Faraday rotation is here the cooperative action of Fe^{3+} ions with degenerate orbital terms that are split further by covalent interaction with Bi^{3+}. In fact, substitution of bismuth results in an overlap between the $6p$ orbit of Bi^{3+}, $2p$ orbit of O^{2-}, and $3d$ orbit of Fe^{3+}. As discussed by Shinagawa,[28] and later by Dionne and Allen,[23] this overlap results in a spin orbit splitting $2\Delta_i$ associated with the tetrahedral and octahedral sites, see also Fig. 5. In the model presented here we ignore the contribution from transitions other than those introduced by bismuth substitution. In fact, LuIG and YIG have very similar Faraday rotation spectra with a positive peak located near 2.8 eV, but with very low Faraday rotation below 2.6 eV.[6] This makes our assumption reasonable.

In order to calculate the magnetooptic response, an expression which links the microscopic parameters to the Far-

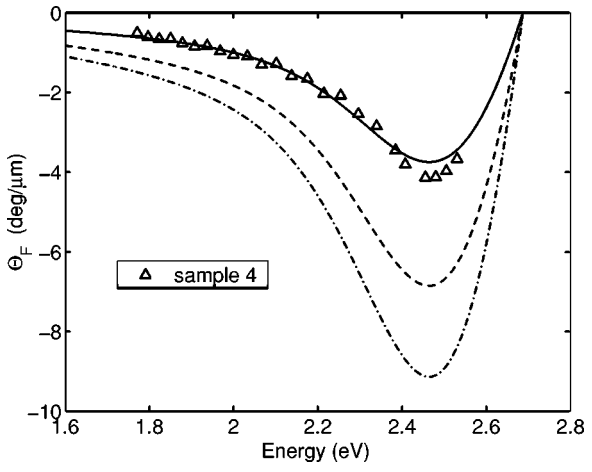

FIG. 4. The Faraday rotation for sample 4. The dashed line represents a theoretical estimate of the Faraday rotation when the gallium substitution is identical to that of sample 4, but with a bismuth substitution of $x=1.5$. The dash-dotted line is similar to the dashed line, but with $x=2$, showing a peak value >9 deg/μm.

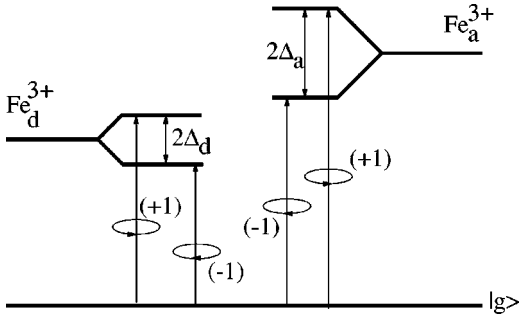

FIG. 5. The basic molecular-orbital energy-level diagram. $(+1)$ and (-1) represents right and left-hand circular polarization, respectively. Note that there are two transitions which influences the Faraday rotation; one associated with the tetrahedral site, the other with the octahedral site. The transitions are assumed to follow the selection rules for electric dipole transitions.

aday rotation is needed. In magnetooptics, this is usually expressed through the complex permittivity tensor, which for Bi:FG has the form

$$\epsilon=\begin{pmatrix} \epsilon_0 & \epsilon_1 & 0 \\ -\epsilon_1 & \epsilon_0 & 0 \\ 0 & 0 & \epsilon_0 \end{pmatrix},$$

where $\epsilon_1=\epsilon_1'+j\epsilon_1''$ represents the magnetooptical response and ϵ_0 the nonmagneto-optical part. In the visible region, the Faraday rotation can be written[24]

$$\Theta_F \approx \frac{\omega}{2nc}\epsilon_1', \tag{2}$$

where ω is the the frequency, or equivalently the energy of the light, c is the speed of light in vacuum, and n is the refractive index. Independent measurements show that it is reasonable to set $n=2.5$ in the visible range.[2,6]

Assuming that the transitions are of electric dipole nature, the off-diagonal elements derived from first order time-dependent perturbation theory are given by[24]

$$\epsilon_1=\frac{2\pi Ne^2}{m}\sum_{i=a,d}\sum_{+}^{-}(\pm)f_{i\pm} \times\frac{\omega(\omega_{i\pm}^2-\omega^2-\Gamma_i^2)+j\Gamma_i(\omega_{i\pm}^2+\omega^2+\Gamma_i^2)}{\omega_{i\pm}(\omega_{i\pm}^2-\omega^2+\Gamma_i^2)^2+4\omega^2\omega_{i\pm}\Gamma_i^2}. \tag{3}$$

The inner sum is over the right- and left-hand circular polarized light, whereas the outer is over the optical transitions in the tetrahedral and octahedral sublattices. The prefactor $(\pm)$ denotes a subtraction. The ω_{i+} and ω_{i-} represent the resonance energy for right and left-hand circular polarized light, respectively. Similarly, f_{i+} and f_{i-} are the respective oscillator strengths, while Γ_i is the half-linewidth of the transition. Furthermore, e and m are the electron charge and mass, respectively, whereas N is the active ion density.

To first order, it is reasonable to assume that N is directly proportional to the bismuth content x.[24] This assumption has

TABLE II. The parameters found to give the best fit between Eq. (7) and the experimental data. Nf_i/x is measured in [cm^{-3}], whereas Δ_i, ω_i and Γ_i are given in [eV]. Note that the tetrahedral and octahedral sites are given different signs, since they contribute oppositely to the Faraday rotation.

site	Nf_i/x				Δ_i	ω_i	Γ_i
	Sample 1	Sample 2	Sample 3	Sample 4			
a	1.72×10^{23}	1.76×10^{23}	1.88×10^{23}	1.69×10^{23}	0.27	3.15	0.47
d	-3.90×10^{22}	-4.00×10^{22}	-4.26×10^{22}	-3.85×10^{22}	0.11	2.51	0.38

also been confirmed by experiments.[6,7] Furthermore, it is known that the strong enhancement of Faraday rotation is caused by iron-pair transitions, involving both octahedral and tetrahedral transitions simultaneously.[30] Therefore, iron dilution of either sublattice results in a reduction of the active ion density. For these reasons we propose that the active ion density can be written as

$$N=N_0(1-u_d/3)(1-u_a/2)x. \tag{4}$$

N_0 is a constant, and may be expected to be 1/3 of the density of rare-earth ions on the dodecahedral site, i.e., 1.3×10^{22} $cm^{-3}/3$. When $x=3$, this interpretation implies that the dodecahedral site is fully occupied by bismuth.

The oscillator strength for right- and left-hand circular polarized light are given by[24]

$$f_{i\pm}=\frac{m\omega_{i\pm}}{2h}|\langle g_i|\hat{X}|e_{i\pm}\rangle|^2, \tag{5}$$

where h is Planck's constant, $\hat{X}$ is the electric dipole operator, and $|g_i\rangle$, $|e_{i\pm}\rangle$ are the wave function of the ground state and excited state, respectively. Using that for the present case one has $\omega_{i\pm}=\omega_i\pm\Delta_i$, we obtain from Eq. (5),

$$f_{i\pm}=\frac{f_i}{2\omega_i}(\omega_i\pm\Delta_i), \tag{6}$$

where f_i is an effective oscillator strength.[24] This expression is based on neglecting the difference between $|e_{i+}\rangle$ and $|e_{i-}\rangle$.

In order to fully predict the Faraday spectra, one needs detailed knowledge about the quantum mechanical oscillator strengths. However, this is not easily accessible with so many ions involved, and we will instead treat them as adjustable parameters in the comparison with experimental data. With Eq. (6) inserted in Eqs. (2) and (3), one obtains

$$\Theta_F=\frac{\pi e^2\omega^2}{nmc}\sum_{i=a,d}\frac{Nf_i}{\omega_i}\left\{\frac{(\omega_i+\Delta_i)^2-\omega^2-\Gamma_i^2}{[(\omega_i+\Delta_i)^2-\omega^2+\Gamma_i^2]^2+4\omega^2\Gamma_i^2}-\frac{(\omega_i-\Delta_i)^2-\omega^2-\Gamma_i^2}{[(\omega_i-\Delta_i)^2-\omega^2+\Gamma_i^2]^2+4\omega^2\Gamma_i^2}\right\}, \tag{7}$$

which represents our model for the Faraday rotation.

IV. DISCUSSION

To fit theoretical curves to the experimental data, the product Nf_i/x was chosen as free parameter. According to Eq. (4) N depends on the gallium and bismuth content. On the other hand, f_i is roughly independent on these two substitutions. Therefore, the product Nf_i/x may be adjusted to any substitutions and transitions. The parameters Δ_i, ω_i, and Γ_i were chosen as sample independent, and the values suggested by Dionne and Allen were used as a starting point in the fitting.[23] Table II presents the parameters we found to give the best fit between the theoretical curves and the experimental data. Note that our values for ω_d, Γ_d and Γ_a differs slightly from those of Dionne and Allen. A reason for this is that the minimum Faraday rotation seems to be shifted slightly towards lower energies as compared to the data analyzed in Ref. 24. Furthermore our values for Γ_d and Γ_a are smaller to account for the narrow linewidth near 2.45 eV seen in Fig. 4.

In Figs. 2 and 3 the Faraday rotation calculated from Eq. (7) is plotted as solid lines, and show an excellent agreement with experimental data. In Fig. 2 the dashed and dash-dotted lines represent the contribution to the total Faraday rotation from the tetrahedral and octahedral sites, respectively. Note that below 2.2 eV, the main contribution to Θ_F comes from the transition related to the octahedral site.

Figure 4 shows the theoretical curve (solid line) fitted to the experimental data for sample 4. Again there is excellent agreement at small photon energies, but some deviation appears above 2.4 eV, where both the experimental and theoretical curves show a peaked behavior. In fact the experimental data indicate a stronger peak than the theoretical prediction. There may be several reasons for such a discrepancy. First, Eq. (4) represents a simplification for the present type of FG's. In particular, we have not considered the canting of the spins or the temperature dependence of N. There is also a possibillity that Δ_i and Γ_i should be chosen differently to obtain a stronger peak around 2.45 eV. Finally, it must be noted that we have neglected the transitions associated with pure LuIG.

We have in Fig. 4 also plotted theoretical predictions for the case $x=1.5$ (dashed curve) and $x=2$ (dash-dotted curve) assuming that gallium content is identical to that of sample 4. When $x=2$ it seems possible to obtain a Faraday rotation exceeding 6 deg/μm at 2.3 eV in this material.

The distribution of gallium on the tetrahedral and octahedral sites have been examined by Czerlinsky and Scott *et al.* for various garnet-compositions with and without bismuth.[29,30] Their results indicated that gallium will replace Fe^{3+} in both tetrahedral and octahedral sublattices, but with the strongest dilution of tetrahedrally coordinated Fe^{3+}. In fact, Czerlinsky found that for $Y_3Fe_4Ga_1O_{12}$ the distribution

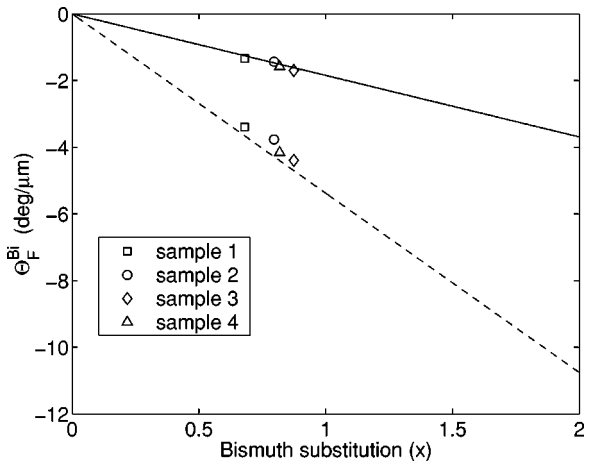

FIG. 6. The Faraday rotation as a function of bismuth content. The experimental points have the same notation as in the previous figures, and are represented for two different energies, 1.97 eV (630 nm) and 2.3 eV (540 nm). The lines are the theoretical curves for the same energies.

is 0.9 Ga on tetrahedral sites and only 0.1 on octahedral sites. Although the samples investigated in this study have somewhat different composition, we will assume that the gallium distribution is the same. Then, based on Eq. (4) the gallium dependence can be removed resulting in a Faraday rotation associated only with the Bi content given by

$$\Theta_F^{\mathrm{Bi}}=\frac{\Theta_F}{(1-u_d/3)(1-u_a/2)}, \tag{8}$$

where $u_d=0.9u$ and $u_a=0.1u$. In Fig. 6 the Θ_F^{Bi} is displayed as a function of the bismuth substitution. The experimental data have the same notation as in the previous figures, and are shown for two different energies, 1.97 eV (630 nm) and 2.3 eV (540 nm), corresponding also to the theoretical curves drawn as solid and dashed lines, respectively. To obtain the theoretical curves we used $N_0 f_a=2.77\times10^{23}$ cm^{-3} and $N_0 f_d=6.30\times10^{22}$ cm^{-3}, which are the average values of the four samples as calculated from Table II and the assumed gallium distribution. The experimental points are located very close to the straight lines, thus indicating that our linear approximation is valid. However, the linear approximation may not hold for large x, since saturation phenomena could change the behavior. In fact, experimental studies by Matsumoto *et al.* indicated breakdown of the linear approximation when $x>2$.[26,27]

V. CONCLUSION

We have synthesized single crystals of bismuth-substituted ferrite garnets by the liquid phase epitaxy method where GGG substrates are dipped into the flux. The growth parameters are controlled to obtain films with in-plane magnetization and virtually no domain activity, which makes them ideally suited for magnetooptic imaging. The Faraday rotation spectra were measured across the visible range of wavelengths. To interpret the spectra we have presented a simple model based on the existence of two optical transitions of diamagnetic character, one tetrahedral and one octahedral. We find excellent agreement with our experimental results within the visible range. It is shown that the Faraday rotation changes significantly with the amount of substituted gallium and bismuth. Furthermore, the experimental results confirm that the magnetooptic response changes linearly with the bismuth substitution. It would be of considerable interest to observe the behavior at low and high temperatures, which will be a topic of future investigations.

ACKNOWLEDGMENTS

We thank Dr. Alexander Solovyev for help to grow samples 1, 2, and 4, and Dr. Muriel Erambert at the Mineral-Geological Museum for assisting in the EMP measurements. This research has been financially supported by the Norwegian Research Council and Tandberg Data ASA.

[1] S. Wittekoek and D.E. Lacklison, Phys. Rev. Lett. **28**, 740 (1972).
[2] S. Wittekoek, T.J.A. Popma, J.M. Robertson, and P.F. Bongers, Phys. Rev. B **12**, 2777 (1975).
[3] H. Takeuchi, Jpn. J. Appl. Phys. **14**, 1903 (1975).
[4] G.S. Krinchik, V.A. Krylova, E.V. Beredennikova, and R.A. Petrov, Sov. Phys. JETP **38**, 354 (1974).
[5] P. Hansen, M. Rosenkrantz, and K. Witter, Phys. Rev. B **25**, 4396 (1982).
[6] P. Hansen, C.P. Klages, J. Schuldt, and K. Witter, Phys. Rev. B **31**, 5858 (1985).
[7] P. Hansen, K. Witter, and W. Tolksdorf, J. Appl. Phys. **55**, 1052 (1984).
[8] P. Hansen, K. Witter, and W. Tolksdorf, Phys. Rev. B **27**, 6608 (1983).
[9] Z. Simsa, J. Simsova, D. Zemanova, J. Cermak, and M. Nevriva, Czech. J. Phys. **34**, 1102 (1984).
[10] A.I. Belyaeva, A.L. Foshchan, and V.P. Yur'ev, Pis'ma Zh. Tekh. Fiz. **17**, 76 (1991) [Sov. Tech. Phys. Lett. **17**, 599 (1991)].
[11] L.A. Dorosinskii, M.V. Indenbom, V.I. Nikitenko, Y.A. Ossip'yan, A.A. Polyanskii, and V.K. Vlasko-Vlasov, Physica C **203**, 149 (1992).
[12] M.R. Koblischka and R.J. Wijngaarden, Supercond. Sci. Technol. **8**, 199 (1995).
[13] A. A. Polyanskii, X. Y. Cai, D. M. Feldmann, and D. C. Larbalestier, *NATO Science Series* Vol. 3/72 (Kluwer Academic Publishers, Dordrecht, 1999), p. 353.
[14] V.K. Vlasko-Vlasov, Y. Lin, U. Welp, G.W. Crabtree, D.J. Miller, and V.I. Nikitenko, J. Appl. Phys. **87**, 5828 (2000).
[15] T.H. Johansen, M. Baziljevich, H. Bratsberg, Y. Galperin, P.E. Lindelof, Y. Shen, and P. Vase, Phys. Rev. B **54**, 16 264 (1996).
[16] A. Hubert and R. Schafer, *Magnetic Domains*, 1st ed. (Springer Verlag, Germany, 1998).
[17] A.N. Egorov and S.V. Lebedev, J. Appl. Phys. **87**, 5362 (2000).

[18] A. Zvezdin and V. Kotov, *Modern Magnetooptics and Magnetooptical Materials* (IOP Publishing, Bristol, 1997).
[19] Z. Simsa, Czech. J. Phys. **34**, 78 (1984).
[20] M. Gomi, H. Furuyama, and M. Abe, J. Appl. Phys. **70**, 7065 (1991).
[21] K. Shinagawa, E. Tobita, T. Saito, and T. Tsushima, J. Appl. Phys. **81**, 1368 (1997).
[22] M. Kucera, J. Kunes, and R. Gerber, J. Appl. Phys. **85**, 5986 (1999).
[23] G.F. Dionne and G.A. Allen, J. Appl. Phys. **75**, 6372 (1994).
[24] G.F. Dionne and G.A. Allen, J. Appl. Phys. **73**, 6127 (1993).
[25] G.A. Allen and G.F. Dionne, J. Appl. Phys. **73**, 6130 (1993).
[26] K. Matsumoto, S. Sasaki, K. Haraga, K. Yamaguchi, and T. Fujii, IEEE Trans. Magn. **28**, 2985 (1992).
[27] K. Matsumoto, S. Sasaki, K. Haraga, K. Yamaguchi, T. Fujii, and Y. Asahara, J. Appl. Phys. **71**, 2467 (1992).
[28] K. Shinagawa, J. Magn. Soc. Jpn. **6**, 247 (1982).
[29] E.R. Czerlinsky, Phys. Status Solidi **34**, 483 (1969).
[30] G.B. Scott, D.E. Lacklison, and J.L. Page, J. Phys. C **8**, 519 (1975).